Design and Evaluation of a Reconfigurable Antenna Array for MIMO Systems

Daniele Piazza, *Student Member, IEEE*, Nicholas J. Kirsch, *Student Member, IEEE*, Antonio Forenza, *Member, IEEE*, Robert W. Heath, Jr., *Senior Member, IEEE*, and Kapil R. Dandekar, *Senior Member, IEEE*

***Abstract*—New reconfigurable antenna array is demonstrated for multiple input multiple output (MIMO) communication systems that improves link capacity in closely spaced antenna arrays. The antenna system consists of an array of two printed dipoles separated by a distance of a quarter wavelength. Each of the dipoles can be reconfigured in length using PIN diode switches. The switch configuration can be modified in a manner adaptive to changes in the environment. The configuration of switches effects the mutual coupling between the array elements, and subsequently, the radiation pattern of each antenna, leading to different degrees of pattern diversity which can be used to improve link capacity. The PIN diode-based reconfigurable antenna solution is first motivated through a capacity analysis of the antenna in a clustered MIMO channel model. A new definition of spatial correlation coefficient is introduced to include the effects of antenna mismatch and radiation efficiency when quantifying the benefit of pattern diversity. Next, the widespread applicability of the proposed technique is demonstrated, relative to conventional half wavelength printed dipoles, using computational electromagnetic simulation in an outdoor and indoor environment and field measurements in an indoor laboratory environment. It is shown for the 2 × 2 system considered in this paper, that an average improvement of 10% and 8% is achieved in link capacity for a signal to noise ratio (SNR) respectively of 10 dB and 20 dB in an indoor environment compared to a system employing non reconfigurable antenna arrays.**

***Index Terms*—Antenna measurements, multiple input multiple output (MIMO) systems, reconfigurable antennas, spatial correlation.**

I. Introduction

MULTIPLE-INPUT multiple-output (MIMO) wireless systems have demonstrated the potential to increase communication spectral efficiency in a rich multipath environment [1]. Recent work in this field has focused on measuring and characterizing the real MIMO propagation channel [2], developing efficient space-time coding strategies [3] and creating novel antenna solutions in order to improve MIMO links [4], [5]. From an antennas perspective, different array configurations and types of element have been proposed and analyzed for MIMO links [4], [5].

It has been shown that signal correlation and mutual coupling effects between MIMO array elements has a significant effect on MIMO capacity [6], [7]. Recently, it has also been shown that pattern diversity, which results from mutual coupling, can potentially lead to low inter-element received signal correlation and thus higher MIMO channel capacity [7], [8].

In this paper, we present a novel reconfigurable MIMO antenna array which will demonstrate how the ability to select between different pattern diversity configurations can improve MIMO system link capacity. The most closely related work [9], [10] has applied this type of reconfigurable antenna to achieve pattern and frequency diversity in &utput (SISO) links. Reconfigurable antennas have also been suggested for application in MIMO systems [11]–[13]. The switch-based parasitic antenna in [14] has also been proposed to improve MIMO system link capacity through pattern diversity. Our reconfigurable antenna solution differs from [14] in that it provides a compact design, suitable for handheld devices.

In this paper, the antenna system under study consists of an array of two reconfigurable microstrip dipoles; the two active elements of the array can be reconfigured in length using PIN diode switches. The setting of the different switches results in different geometries of the antenna and, as a result, different levels of inter-element mutual coupling and array far-field radiation patterns. The goal of such a system is to choose the configuration of switches in a environment/channel adaptive fashion to decrease MIMO spatial channel correlation and subsequently maximize link capacity.

The proposed reconfigurable antenna system was used to implement a 2 × 2 MIMO system employing spatial multiplexing transmission. The benefits derived from using our reconfigurable MIMO antenna system is first motivated through spatial correlation coefficient analysis in a clustered MIMO channel model [15]. Through this analysis, we demonstrate the advantage of switching between different antenna configurations based on the spatial characteristics of the MIMO channel. In conducting this analysis, we developed a new definition of spatial correlation to include the effects of antenna mismatch and radiation efficiency when quantifying the impact of pattern diversity on MIMO systems. Since some limitations with the adopted clustered channel model have been recognized (i.e. underestimation of actual MIMO channel capacity and consideration of azimuthal radiation pattern instead of full 3D radiation) [16]–[18], in this paper, we verify the performance

Manuscript received July 27, 2006; revised April 15, 2007. This work was supported by the National Science Foundation under Grants 0435041 and 0322795.

D. Piazza, N. J. Kirsch, and K. R. Dandekar are with the Department of Electrical and Computer Engineering, Drexel University, Philadelphia, PA 19104-2875 USA (e-mail: dp84@drexel.edu; njk27@drexel.edu; dandekar@drexel.edu).

A. Forenza is with Rearden, LLC, San Francisco, CA 94107 USA (e-mail: antonio@rearden.com).

R. W. Heath, Jr., is with the Department of Electrical and Computer Engineering, The University of Texas at Austin, TX 78712 (e-mail: heath@ece.utexas.edu).

Color versions of one or more of the figures in this paper are available online at http://ieeexplore.ieee.org.

Digital Object Identifier 10.1109/TAP.2008.916908

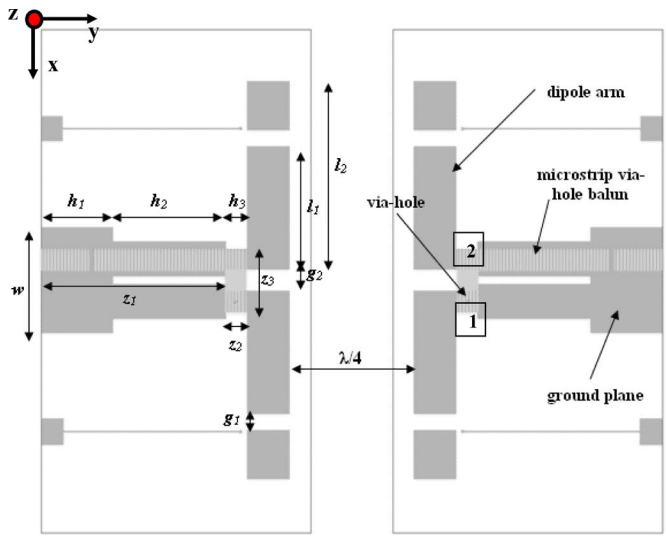

Fig. 1. Dipole antenna design.

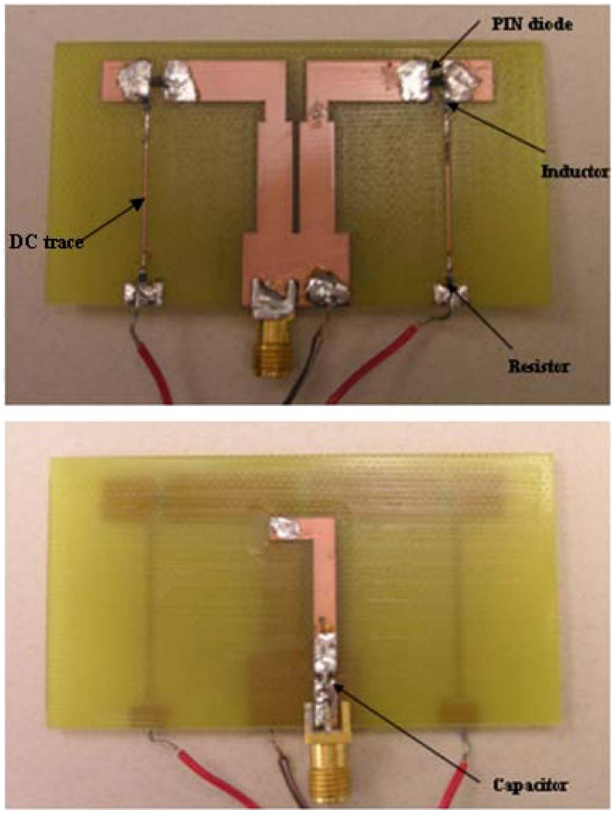

Fig. 2. Antenna structure: top and bottom view.

of the proposed reconfigurable antenna using both *i*) computational electromagnetic simulation (simulation technique described in [19]) in outdoor and indoor environment, and *ii*) experimental field-testing in an indoor environment. In conducting this analysis the two antennas have been assumed to transmit/receive simultaneously including therefore the effects caused by the superposition of the antenna's radiation patterns at the receiver and transmitter.

This paper is organized as follows. In Section II, we introduce the MIMO channel model used to evaluate the reconfigurable antenna array. In Section III, the physical parameters of the reconfigurable antenna system design and radiation pattern simulations are presented. In Section IV, a new formulation of spatial correlation coefficient for quantifying MIMO pattern diversity is presented. This spatial correlation analysis in a MIMO clustered channel model motivates the use of the proposed reconfigurable antenna in MIMO systems. In Section V, simulation results are presented for the proposed antenna obtained using computational electromagnetic simulations in an outdoor environment. In Section VI we analyze capacity results from field-measurements taken on a 2×2 MIMO testbed using the reconfigurable MIMO array, and we compared them with results obtained with computational electromagnetic simulations performed in the same indoor environment. Finally, conclusions are drawn in Section VII.

II. MIMO System and Channel Model

In a narrowband MIMO wireless system with N_t transmit antennas and N_r receive antennas, the signal collected at the receiver is related to the signal outgoing from the transmitter through the relation

$$\mathbf{y} = \mathbf{H}\mathbf{x} + \mathbf{n} \tag{1}$$

where $\mathbf{y} \in C^{N_r \times 1}$ is the signal vector at the receiver array, $\mathbf{x} \in C^{N_t \times 1}$ is the signal vector at the transmit antenna array, $\mathbf{n} \in C^{N_r \times 1}$ is the complex additive white Gaussian noise (AWGN) vector and $\mathbf{H} \in C^{N_r \times N_t}$ is the channel transfer matrix. Assuming that the channel is unknown at the transmitter and known at the receiver, the signal vector at the transmitter is composed of N_t independent signals with equal power. In this case, the capacity is given by [20]

$$C = \log_2 \left[\det \left(\mathbf{I}_{N_r} + \frac{SNR}{N_t} \mathbf{H}\mathbf{H}^{\dagger} \right) \right] \tag{2}$$

where $\mathbf{I}_{N_r}$ is an $N_r \times N_r$ identity matrix, $\dagger$ denotes a complex conjugate transpose operation, and SNR is the average signal-to-noise-ratio over all receiver array elements.

In a correlated Rayleigh-fading MIMO channel the channel matrix $\mathbf{H}$ is defined, according to the Kronecker model [21], [22], as

$$\mathbf{H} = \mathbf{R}_r^{1/2} \mathbf{H}_w \mathbf{R}_t^{1/2} \tag{3}$$

where $\mathbf{R}_t$ and $\mathbf{R}_r$ denote respectively the transmit and receive spatial correlation matrices and $\mathbf{H}_w \in C^{N_r \times N_t}$ is a matrix of complex Gaussian fading coefficients. In this paper, the special case of $N_t = N_r = 2$ is considered.

The "Kronecker" model [21] in (3) is adopted in this paper to illustrate the potential of the proposed reconfigurable antenna. The same model has been used previously in the literature [8] to demonstrate the benefits of pattern diversity in MIMO communication systems.

The spatial correlation coefficients (entries of the matrix $\mathbf{R}_t$ and $\mathbf{R}_r$) and the channel capacity can be generated through a clustered MIMO channel as described in [23]. In clustered MIMO channel models, the scattering objects around the transmit/receive arrays are modeled as "clusters". Each cluster is characterized by a mean angle of arrival (AOA) Ω_c, where

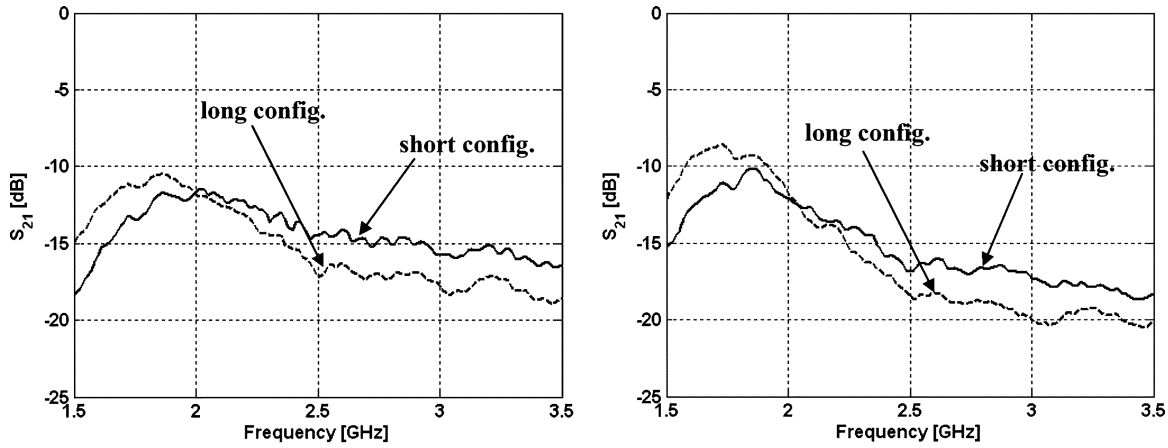

Fig. 3. The measured S_{21} for the "long" and "short" antenna configuration in a 2 element array with inter-element separation of $\lambda/4$ when (a) the other antenna is in the "short" configuration, and (b) the other antenna is in the "long" configuration.

$\Omega_c = (\phi_c, \theta_c)$ represents the solid angle consisting of azimuth (ϕ_c) and elevation (θ_c) components. For simplicity, it is assumed that there is a single cluster (as in [8]) and that the cluster location is distributed only over azimuth directions with mean AOA, ϕ_c (as in [8] and [23]). Depending on the system bandwidth, the excess delay across different propagation paths may not be resolvable. In this case, multiple AOAs are defined with an offset ϕ with respect to the mean AOA of the cluster (ϕ_c). This angle of arrival is generated according to a certain probability density function (PDF) that models the power angular spectrum (PAS). The variance of the PAS is a measure of the angle spread (AS), σ_ϕ, of the cluster.

III. Antenna Design

The proposed antenna solution has been realized using an array of two microstrip dipoles [24], the geometry of which is shown in Fig. 1 and Fig. 2. A quarter-wavelength microstrip balun acts as an unbalanced-to-balanced transformer from the feed coaxial line to the two printed dipole strips [25]. The ground plane of the microstrip line and the dipole strips are in the same plane. As indicated in this figure, the presence of a via-hole permits feed point 2 of a printed dipole strip to be shifted in phase by 180° with respect to the feed point 1 of the other printed dipole strip. This occurs because of the 180° phase difference between the top strip and the ground plane of the microstrip line.

The lengths of the dipole-arm strip, and therefore the geometry of the antenna, can be changed using two PIN diode switches (MA4P789), which guarantee an isolation of 36 dB and low insertion loss (0.7 dB). In this way, it is possible to define two configurations for the antenna, one when both of the switches are turned on ("long" configuration) and another when they are turned off ("short" configuration). In order to drive the switches, a direct bias voltage of 1.7 V is supplied to the diode with two thin traces, the presence of which, as analyzed through electromagnetic simulations, does not corrupt the radiation characteristics of the antenna. A surface mounted capacitor of 47 pF is placed on the balun to block the dc current from flowing back to the RF input, an inductor of 56 nH is used to block the RF from flowing in the dc supply trace, and a resistor of 100 Ω is mounted to limit the voltage across the diode as shown in Fig. 2. The structural parameters of the printed dipole antenna are listed in the Table I.

TABLE I
List of Structural Parameters of the Printed Dipole Antenna

PCB substrate	thickness	$1.5\,mm$
	ϵ_r	4.4
	$tan\,\delta$	0.0018
dipole arm	l_1	$19\,mm$
	l_2	$28\,mm$
	w	$6\,mm$
	g_1	$2.6\,mm$
	g_2	$3\,mm$
microstrip balun	z_1	$29\,mm$
	z_2	$3\,mm$
	z_3	$9\,mm$
via-hole	radius	$0.4\,mm$
ground plane	h_1	$10\,mm$
	h_2	$16\,mm$
	h_3	$3\,mm$
	h_4	$15\,mm$

The antenna structure has been analyzed and simulated using the method of moments (MoM) (FEKO software) [26]. The behavior of the switch has been modeled using a microstrip line with the same scattering parameters of the PIN diode in both ON and OFF configurations.

The close proximity of the two printed dipoles has been selected such that there is a strong mutual coupling between the two dipoles. This coupling is effectively used to have different radiation patterns for each array's geometry. In particular because of the vicinity of the two reconfigurable dipoles, varying the length of one of the dipoles, effects the input impedance and the current distribution of the other dipole, changing therefore its radiation properties [25]. Fig. 3 shows the coupling level between the different possible configurations of antenna geometry in an array (both "short," both "long," first antenna "short" and second "long," first antenna "long" and second "short"). It can

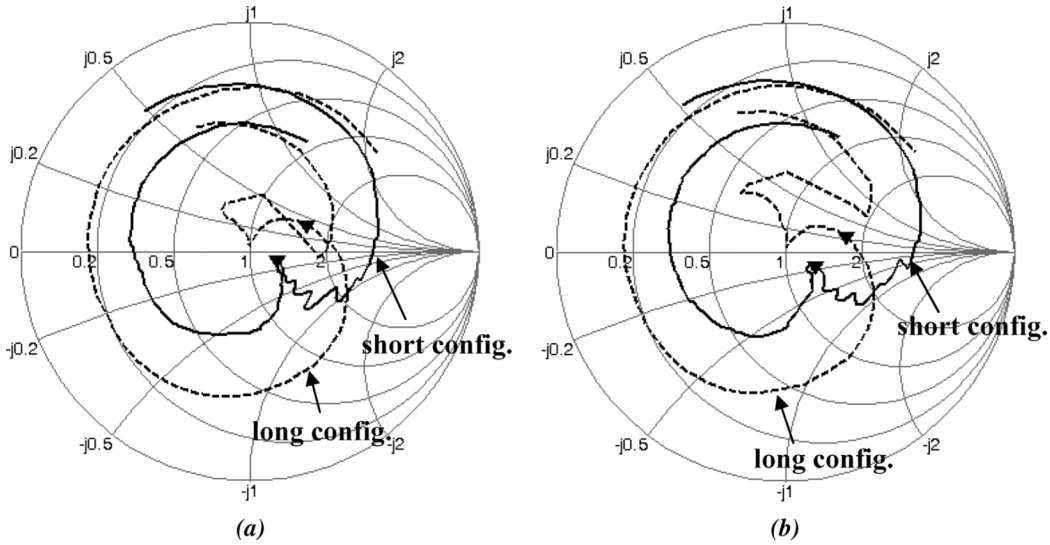

Fig. 4. The measured antenna input impedance for the "long" and "short" antenna configuration in a 2 element array with inter-element separation of $\lambda/4$ for frequencies from 1.5 GHz to 3.5 GHz when (a) the other antenna is in the "short" configuration, and (b) the other antenna is in the "long" configuration. A marker selects the frequency of 2.45 GHz.

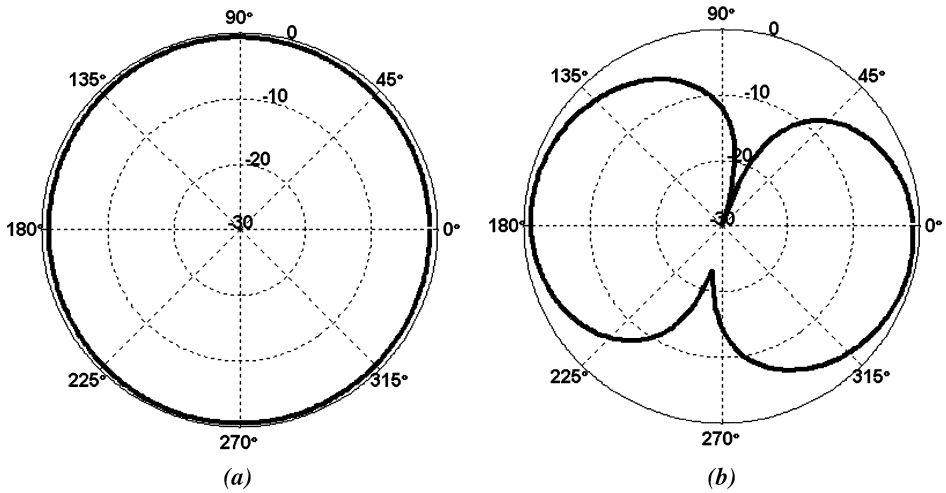

Fig. 5. Radiation pattern (in dB) in the E plane (a) and in the H plane (b) of the printed dipole in the "short" configuration for an operation frequency of 2.45 GHz.

be noted that the mutual coupling is different for each configuration of the array. In Fig. 4 is depicted the input impedance of one of the two dipoles for each array configurations. It can be noted that the reconfigurable dipole is characterized by an input impedance that is different for each array's configuration. These differences in input impedance are due to the different lengths of the dipole and the different level of mutual coupling of each configuration. A difference in input impedance is in fact observed not only when the "active" dipole length is changed from "short" to "long" but also when the "parasitic" dipole length is changed from "short" to "long" leaving the "active" dipole length unchanged.

The strong mutual coupling effects between the two antennas influence also the radiation propertied of the array's elements. Fig. 5 shows the simulated radiation pattern of a single element half wavelength printed dipole. The radiation pattern is greatly modified when the antenna is used in a two element array with inter element separation of $\lambda/4$. For the different possible configurations of antenna geometry in an array (both "short", both "long", first antenna "short" and second "long", first antenna "long" and second "short") the simulated radiation pattern of the two elements is reported in Fig. 6 and Fig. 7 in the H and E planes for the operation frequency of 2.45 GHz. The radiation pattern of each dipole configuration is measured leaving the other dipole of the array open circuited according to [27]. The radiation pattern, which is linearly polarized, changes from one configuration to another. Fig. 6 shows the main differences in radiation pattern between the different antenna configurations. In particular the plot shows that the "long" configuration has a more prominent secondary lobe than the "short" configuration. This difference also makes the "short" configuration more directive than the "long" configuration. Another difference between configurations is in the direction of the main beam. In Fig. 6(b) and Fig. 6(c), the radiation patterns are tilted $5^\circ - 10^\circ$ with respect to the radiation patterns in Fig. 6(a) and Fig. 6(d). Fig. 7 does not show as many differences in the patterns between con-

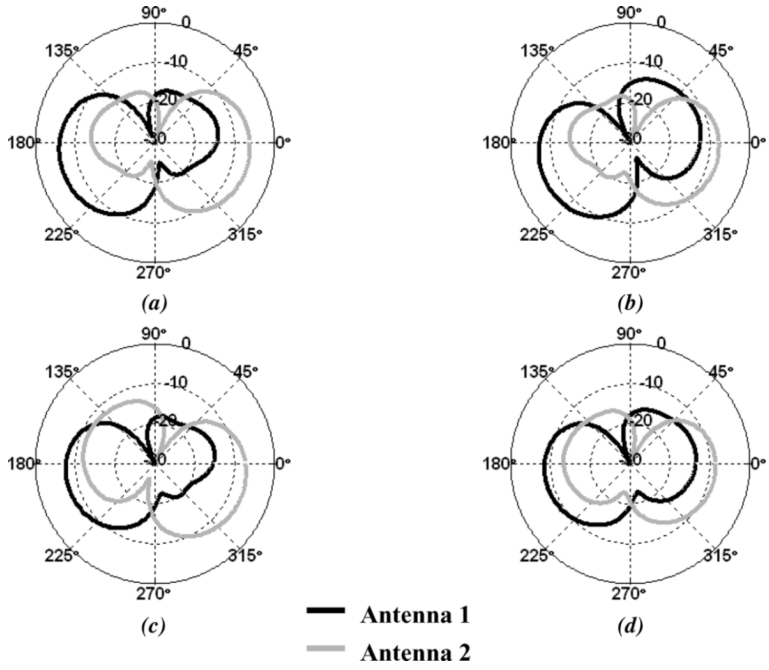

Fig. 6. Radiation pattern (in dB) in the H plane ($\theta = 90°$) of the two printed dipole separated by $\lambda/4$ in all the configurations for an operation frequency of 2.45 GHz: (a) antenna 1, "short," antenna 2, "short;" (b) antenna 1, "long," antenna 2, "short;" (c) antenna 1, "short," antenna 2," long;" (d) antenna 1, "long," antenna 2, "long".

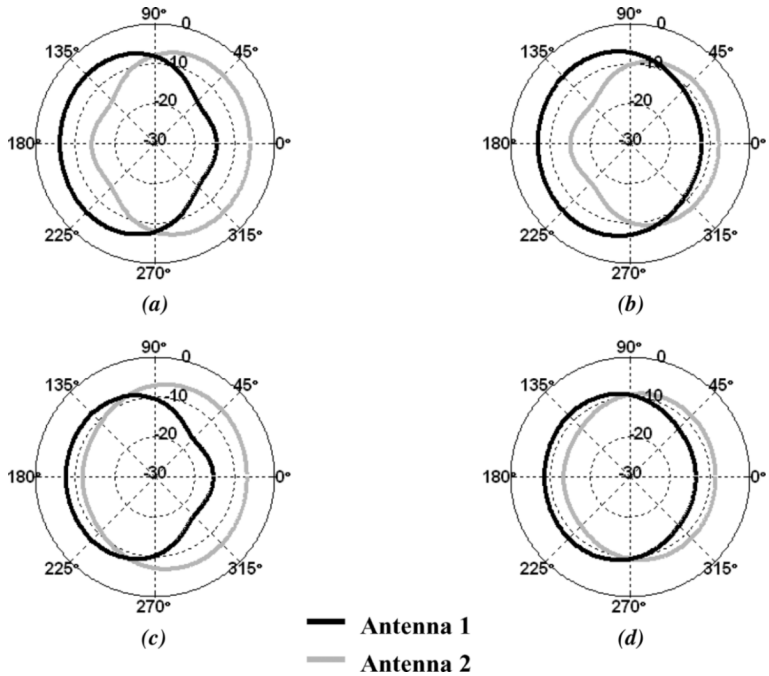

Fig. 7. Radiation pattern (in decibels) in the E plane ($\phi = 90°$) of the two dipole separated by $\lambda/4$ in all the configurations for an operation frequency of 2.45 GHz: (a) antenna 1, "short," antenna 2, "short;" (b) antenna 1, "long," antenna 2, "short;" (c) antenna 1, "short," antenna 2," long;" (d) antenna 1, "long," antenna 2, "long."

figurations as Fig. 6, however the difference in directivity can be observed. Fig. 6 and Fig. 7 also show the different levels of radiated power (i.e., efficiencies) between the four possible array configurations.

The simulated as well as the measured values of the return loss of the antenna in the two configurations are shown in Fig. 8. The return loss for the antenna is determined when the antenna is placed in a two element array with inter-element spacing of $\lambda/4$ so that the effects of mutual coupling can be incorporated into the antenna input impedance. The system has been designed to work in the frequency band between 2.4 GHz and 2.48 GHz typical of an 802.11-like MIMO-aware WLAN and Fig. 8 shows

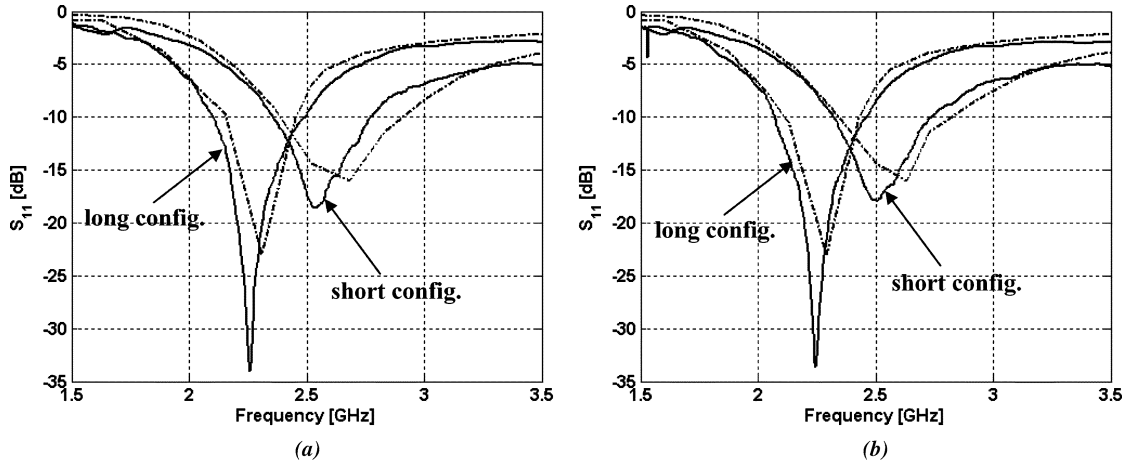

Fig. 8. The measured reflection coefficient for the "long" and "short" antenna configuration in a 2 element array with inter-element separation of $\lambda/4$ when (a) the other antenna is in the "short" configuration, and (b) the other antenna is in the "long" configuration. The respective simulated curves are also shown dashed.

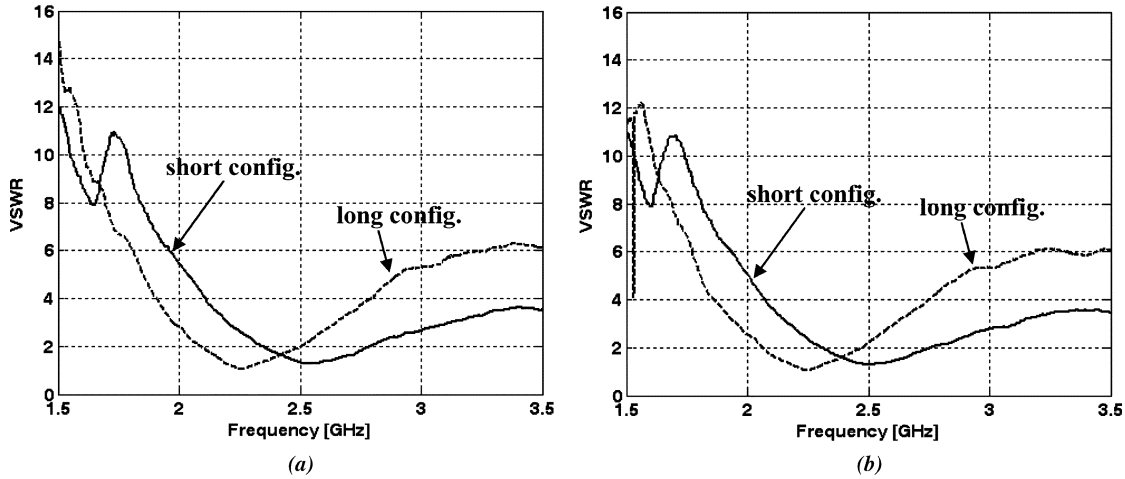

Fig. 9. The measured VSWR for the "long" and "short" antenna configuration in a 2 element array with inter-element separation of $\lambda/4$ when (a) the other antenna is in the "short" configuration, and (b) the other antenna is in the "long" configuration.

that the antenna configurations are matched at the frequency band of interest (for a target S_{11} of -10 dB). In particular the "short" configuration (half wavelength microstrip dipole) performed better than the "long" configuration (three quarter wavelength microstrip dipole) both in radiation efficiency η ("long" configuration $\eta = 62\%$, "short" configuration $\eta = 75\%$) and in matching condition. In Fig. 9 is then shown the measured $VSWR$ for all the array's configuration, from which it is evident that each antenna's configuration is matched over the bandwidth of interest.

The proper choice of the receiver and transmitter array switch configurations (i.e. the length of each antenna) is the one which decreases MIMO spatial channel correlation and maximizes channel capacity for a particular multipath environment. For example, the optimal choice could be determined by switching through all the possible length configurations at transmitter and receiver whenever the capacity experienced by the link falls below a predefined threshold. The scope of this paper is to demonstrate proof-of-concept capacity improvements in static networks in indoor and outdoor environments.

IV. Antenna Analysis in Clustered MIMO Channel Model

In this section, we propose a new definition of spatial correlation to quantify the only pattern diversity while including the effects of antenna input impedance and radiation efficiency. Using this new definition, the proposed reconfigurable antenna array for MIMO systems is motivated through spatial correlation and ergodic capacity performance analysis in clustered channels.

A. Spatial Correlation Coefficients

The spatial correlation between the lth and mth elements of MIMO arrays, previously used to quantify pattern diversity is given by [23]

$$r_{l,m} = \frac{\int_{4\pi} P(\Omega)\underline{E}_l(\Omega)\underline{E}_m^*(\Omega)d\Omega}{\int_{4\pi} P(\Omega)\left|\underline{E}_{iso}(\Omega)\right|^2 d\Omega} \tag{4}$$

where $\Omega = (\phi, \theta)$ is the solid angle, $P(\Omega)$ is the PAS of the scattered fields, $\underline{E}_l(\Omega)$ is the far-field radiation pattern of the l-th antenna of the reconfigurable antenna array and $\underline{E}_{iso}(\Omega)$ is the

far-field radiation pattern of ideal isotropic radiators. Moreover, it is assumed that

$$\int_{4\pi} P(\Omega)d\Omega = \int_{4\pi} \left|\underline{E}_l(\Omega)\right|^2 d\Omega = \int_{4\pi} \left|\underline{E}_{iso}(\Omega)\right|^2 d\Omega = 1 \quad (5)$$

where the first term of the equality is the condition for $P(\Omega)$ to be a PDF.

Since the spatial correlation is normalized with respect to the antenna gain of ideal isotropic radiators, the envelope of (4) is not guaranteed to be lower than one, as provided by the conventional definition of correlation [28], [29]. This guarantee cannot be satisfied because in (4) the power radiated by the isotropic radiator and the lth and mth elements of the MIMO arrays are assumed to be equal. For the case of the proposed reconfigurable antenna, however, the above assumption does not hold because each antenna configuration has different levels of radiated power given equal input power. This difference in radiated power occurs because of the different input impedance and efficiency of each configuration, as shown in Section III.

In order to model the effects of antenna radiation efficiency and input impedance, the definition in (4) has been revised

$$r_{l,m} = \sqrt{\left(1-\left|S_{11_l}\right|^2\right)\eta_l \left(1-\left|S_{11_m}\right|^2\right)\eta_m} \times \frac{\int_{4\pi} P(\Omega)\underline{E}_l(\Omega)\underline{E}_m^*(\Omega)d\Omega}{\int_{4\pi} P(\Omega)\left|\underline{E}_{iso}(\Omega)\right|^2 d\Omega} \quad (6)$$

where S_{11_l} and S_{11_m} are the voltage reflection coefficients at the lth and mth antenna input ports and η_l and η_m describe the percentage of power lost due to ohmic and dielectric losses in the respective antennas. Note that in this definition of spatial correlation coefficient the radiation pattern of an array element is defined for a unit driving current and all other elements in the array terminated in an open circuit.

We observe that the definition in (6) accounts for the cross-polarization components of the radiated/incident fields. In fact, from equation (4) in [29], we define the PAS as $P(\Omega) = P_\phi(\Omega) + P_\theta(\Omega)$, where P_ϕ and P_θ are the angular power densities of the $\hat{\phi}$ and $\hat{\theta}$ components of the incident field, respectively. For the sake of simplicity it is assumed $P_\phi(\Omega) = P_\theta(\Omega) = P'(\Omega)$, which is equivalent to say that the channel is characterized by a unitary cross-polarization-discrimination ($XPD = 0$ dB) as defined in [29], [30]. Thus $P(\Omega) = P_\phi(\Omega) + P_\theta(\Omega) = 2P'(\Omega)$. It is also assumed, consistent with the measurements results in [31], that most of the scattered power propagates over the azimuth directions. Therefore $P(\Omega) = 2P'(\Omega) = Q(\Omega) * \delta(\phi - \phi_c)\delta(\theta - \pi/2)$, where $*$ denotes the convolution operator, ϕ_c is the mean AOA of the cluster and $Q(\Omega)$ is generated according to the truncated Laplacian distribution as in [15].

B. Performance in Clustered MIMO Channel Model

In this section, we evaluate the capacity performance of the proposed reconfigurable antenna in clustered MIMO channel models described in Section II. The capacity is computed from the spatial correlation coefficients defined in (6).

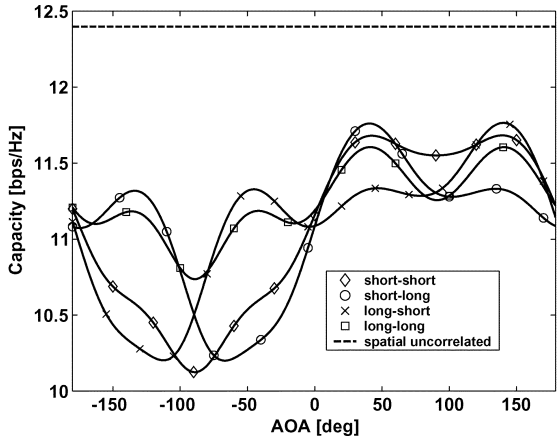

Fig. 10. Single-sided correlated MIMO channel ergodic capacity for the four possible array configurations as a function of the cluster mean AOA, with $\mathrm{SNR} = 20$ dB. The erogdic capacity for a double-sided uncorrelated channel is also shown as a reference.

The spatial correlation coefficients were numerically evaluated by employing realistic radiation patterns in the azimuthal plane (see Fig. 6) for all the switch configurations of a two element reconfigurable antenna array. The MIMO channel capacity was computed by using the spatial correlation coefficients in (6). A tight upper bound on the ergodic capacity for spatial multiplexing systems (with equal power allocation across the transmit antennas) [32], was adopted in this paper. The upper bound for double sided correlated MIMO channel capacity is expressed as

$$C \le log_2\left[\sum_{k=0}^{N_{min}}\left(\frac{SNR}{N_t}\right)^k k! \sum_{1\le i_1<i_2\ldots<i_k\le N_t}\left|\mathbf{R}_{t_{i_1,i_2,\ldots,i_k}}^{i_1,i_2,\ldots,i_k}\right| \times \sum_{1\le i_1<i_2\ldots<i_k\le N_r}\left|\mathbf{R}_{r_{i_1,i_2,\ldots,i_k}}^{i_1,i_2,\ldots,i_k}\right|\right] \quad (7)$$

where $N_{min} = min(N_r, N_t)$ and $|\mathbf{R}_{t_{i_1,i_2,\ldots,i_k}}^{i_1,i_2,\ldots,i_k}|$, $|\mathbf{R}_{r_{i_1,i_2,\ldots,i_k}}^{i_1,i_2,\ldots,i_k}|$ are the minor determinants of $\mathbf{R}_t$ and $\mathbf{R}_r$ (i.e., a determinant of the $k \times k$ matrix lying in the $i_1, i_2, \ldots, i_k$ rows and in the $i_1, i_2, \ldots, i_k$ columns of $\mathbf{R}_t$ and $\mathbf{R}_r$.

We first considered the performance of the reconfigurable array in single-sided correlated MIMO channels. In single-sided correlated channels, either $\mathbf{R}_t = \mathbf{I}$ or $\mathbf{R}_r = \mathbf{I}$, with the other matrix determined by the clustered MIMO channel model. Thus, the channel capacity was computed for a MIMO system employing the reconfigurable antenna at only one end of the link. Fig. 10 shows the channel capacity achieved with the four possible array configurations as a function of the mean AOA (ϕ_c) of the cluster, for an angular spread of $\sigma_\phi = 30°$ and $SNR = 20$ dB. Fig. 10 also shows the capacity of a double-sided uncorrelated 2×2 MIMO channel ($\mathbf{R}_t = \mathbf{R}_r = \mathbf{I}$) as a reference. It can be observed that for each antenna configuration, the capacity varies over the mean AOA of the cluster. The highest value of achievable capacity can be guaranteed by switching between the four array configurations, since each configuration outperformed the others in certain mean AOA ranges.

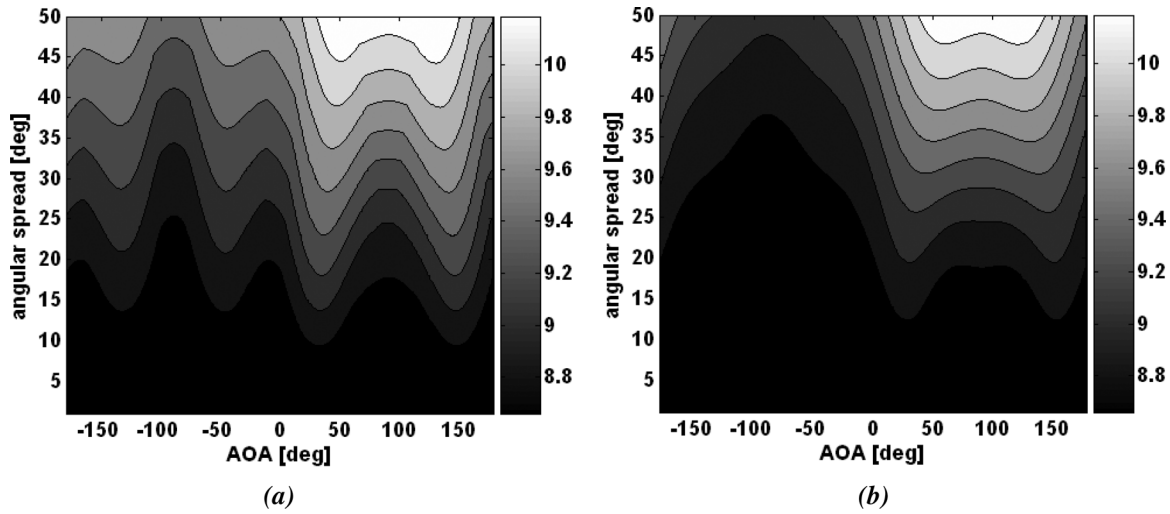

Fig. 11. Contour plot of the double-sided correlated MIMO channel ergodic capacity for the (a) reconfigurable antenna array, and of the (b) non-reconfigurable $\lambda/2$ printed dipole as a function of the cluster mean AOA and per-cluster AS, with $SNR = 20$ dB.

In order to complete a channel capacity analysis of the reconfigurable antenna in a clustered channel model, the channel capacity defined in (7) was computed for a double sided correlated channel (i.e. both $\mathbf{R}_t$ and $\mathbf{R}_r$ determined by the clustered MIMO channel model). In this case, the proposed reconfigurable antenna was used at both ends of the MIMO link. The capacity of the channel was found according to (7) for each possible configuration of the transmitting and receiving antenna array, for a total of 16 different configurations. The capacity achievable with the reconfigurable antenna array was defined as the highest one among the 16 antenna configurations. Fig. 11(a) depicts the double-sided correlated MIMO channel ergodic capacity of the reconfigurable antenna as a function of the cluster mean AOA and cluster angle spread (assuming these parameters to be the same at both the transmitter and the receiver side), with $SNR = 20$ dB. In Fig. 11(b) the ergodic capacity achievable with the same printed dipole in the "short" configuration (as specified previously, the most efficient in terms of radiation and matching) is reported as a reference non-reconfigurable antenna system. The results show the variation of the capacity with the mean AOA of the cluster and the AS. The reconfigurable antenna outperforms the non reconfigurable printed dipole for every mean AOA and every AS. With respect to the single-sided correlated channel of Fig. 10, the situation in Fig. 11(a) shows the capacity achieved is lower, since both transmitter and receiver sides are correlated. However, the double-sided correlated channel better describes the real channel when closely spaced antenna array elements are used. Moreover, the relative capacity improvement achievable with the reconfigurable antenna in a double-sided correlated channel is higher than the capacity improvement achievable in a single-sided correlated channel.

The obtained results motivate then the use of this reconfigurable antenna in a MIMO link and demonstrate how a decision rule for switching configuration can be generated using the information of the channel spatial correlation, that is a function of mean AS and AOAs.

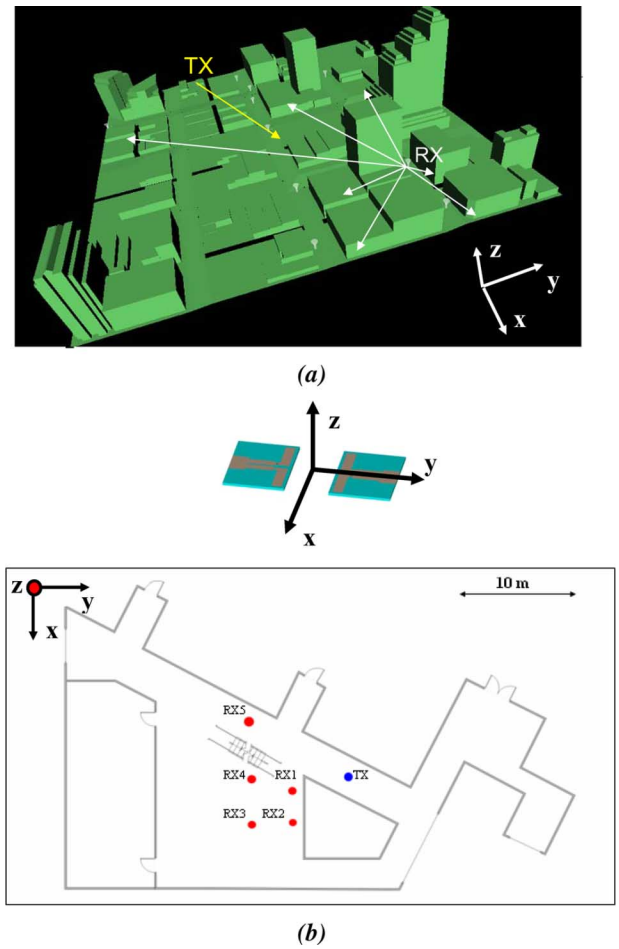

Fig. 12. Outdoor and indoor environments models: (a) 3D model of downtown Austin (TX location is shown with some of the RX locations), (b) orientation of reconfigurable antenna array in the indoor environment illustrating the multiple receiver locations and the transmitter location.

Since some limitations with the adopted clustered channel model have been recognized [16]–[18], in the next two sec-

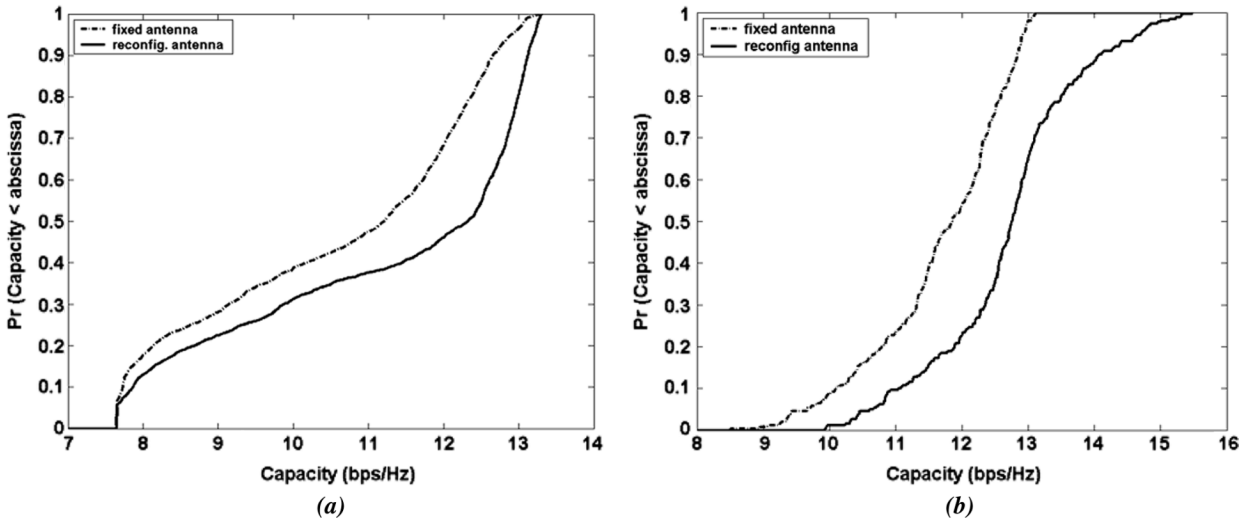

Fig. 13. CDF of capacity for the reconfigurable and fixed antenna array in a (a) ray tracing simulated outdoor environment, and in a (b) measured indoor environment.

tions, the reconfigurable antenna performance is analyzed using computational electromagnetic simulation in an outdoor and indoor environment, and experimental field-testing in an indoor environment. In particular through electromagnetic simulations and experimental field-testing the effect of considering the full 3D antenna radiation pattern is investigated in realistic environments that consist of more than one cluster and in which the effect of cross-polarization is considered.

V. Ray Tracing Simulation Results

In this section, the reconfigurable antenna array is studied in terms of channel capacity, via numerical computation using an electromagnetic ray tracer, FASANT [33]. FASANT is a deterministic ray tracing program based on geometric optics and the uniform theory of diffraction. A 3D model of Austin downtown was simulated as the geometry input of FASANT. There was a transmission point located in the center of the model, at a height of 1.5 m, and a receiver, at a height of 1.5 m, moving along the streets, as shown in Fig. 12(a), occupying 2400 different locations. Note that the orientation of the array has been selected such that the maximum degree of pattern diversity between the different antenna's configuration is in the azimuthal plane.

The radiation patterns (Fig. 6 and Fig. 7), obtained from FEKO antenna design software, for the different configurations of the antenna spaced by $\lambda/4$ were used in the ray tracing simulation both at the receiver as well as at the transmitter in a 2×2 MIMO system. Ray tracing considers the effects caused by the superposition of the antenna's radiation patterns at the receiver and transmitter.

The channel matrix $\mathbf{H}$ was computed as described in [34]. To define the capacity of the MIMO communication link, a Frobenius normalization of the channel matrix was computed in order to remove the differences in path loss among a number of channel matrices [35]. Specifically, to preserve the relative antenna gain effects of each configuration, all the channel matrices for each receiver location were normalized with respect

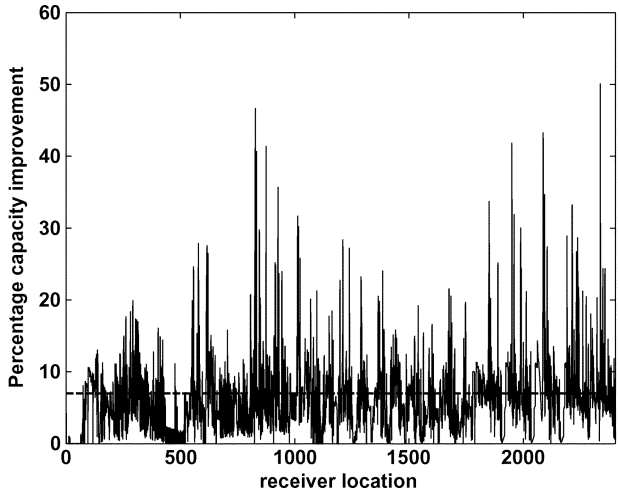

Fig. 14. Percentage capacity improvement achieved with the reconfigurable antenna versus receiver location, and mean percentage capacity improvement (dashed line) in outdoor environment.

to the "short" configuration channel matrix. The normalization factor N_F is defined as:

$$N_F = \sqrt{\frac{\|\mathbf{H}_{\text{“}short\text{"}}\|_F^2}{N_t N_r}} \tag{8}$$

The capacity of the link was then determined using (2), assuming a SNR of 20 dB.

The capacity of the channel was found in this way for each possible configuration of the transmitting and receiving antenna array, for a total of 16 different configurations per position, and the optimal solution of the reconfigurable antenna was the one which guaranteed the highest channel capacity. The channel capacity achieved using the reconfigurable antenna was compared with the capacity of a MIMO link where the same printed dipole in the "short" configuration (as specified previously to be the most efficient in terms of radiation and matching) was

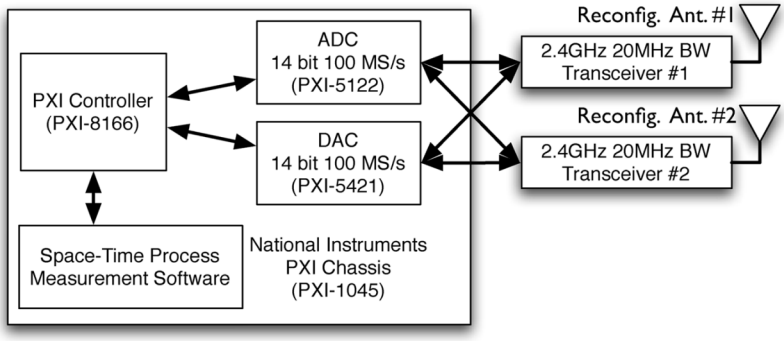

Fig. 15. MIMO OFDM testbed block diagram.

used at the transmitter and receiver array. Based on the data collected from simulations, a cumulative distribution function (CDF) for the capacity was numerically obtained and shown in Fig. 13(a), where one curve represents the CDF relative to a system where the reconfigurable antenna solution was used, and the other was relative to one where the "short" configuration (fixed antenna) was used. The percentage improvement in capacity that the system provided on a location-by-location basis, with respect to the fixed antenna solution, is shown in Fig. 14. As shown by the dashed line the average percentage improvement in capacity results is 7% for a SNR of 20 dB, reaching peaks of 40% for certain receiver positions. It can also be observed, as shown in Section IV, that the operation of the system was dependent on the particular environment between the transmitter and the receiver.

VI. Measurements Results

The proposed reconfigurable antenna was then tested taking measurements on a 2×2 MIMO orthogonal frequency division multiplexing (OFDM) testbed communication system in an indoor environment. Each node of the experimental platform consisted of frequency agile transceivers operating in the ISM and UNII radio bands and a baseband process computer. The baseband chassis provided by National Instruments had two major functional roles. First, the unit contained the analog to digital (A/D) and (D/A) converters required for the two transceivers. The converters operated at 100 MS/s with 14-bit quantization. Second, the baseband unit was a software defined radio (SDR) which allowed the physical layer to be flexible in implementing different experiments. An overview of the testbed can be seen in Fig. 15.

Two nodes have been used for measurement. As shown in Fig. 12(b), the measurements were taken in the hallway of the 3rd floor of the Bossone Research building on Drexel University campus. The transmitter was stationary, while the receiver was moved between several different locations. The channel matrix was measured for 5 different locations of the receiver and for all 16 possible configurations of the antenna system. The measurements were performed at 2.484 GHz. We used BPSK to generate the analog baseband signal. The analog signal obtained was modulated using OFDM with the data being sent on each of the 52 sub-carriers. The spacing between each sub carrier was 312.5 kHz. A training pattern using binary phase shift keying

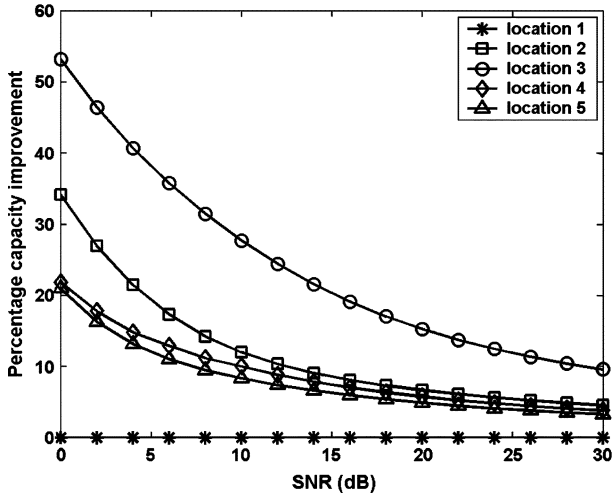

Fig. 16. Percentage capacity improvement versus SNR for 5 different receiver locations in indoor environment (improvement defined as the normalized difference in capacity between the best configuration between the sixteen possible solutions of the reconfigurable antenna system and a 2×2 MIMO system with fixed length antennas).

(BPSK) was transmitted independently over the two transmitters. This training pattern was then received and used to estimate the channel matrix [36]. The orientation of the array, depicted in Fig. 12(b), has been selected such the maximum degree of pattern diversity between the different antenna's configuration is in the azimuthal plane.

To determine the capacity of the MIMO wideband communication link, a normalization of the channel matrix for each sub-carrier was computed using the Frobenius norm as described in Section IV, in order to remove the differences in path loss among a number of channel matrices [35]. Specifically, all the channel matrices for each receiver location and for each sub-carrier was normalized with respect to the "short" configuration channel matrix at the respective location and sub-carrier.

The capacity of the link was then determined using the equation

$$C = \frac{1}{m}\sum_{i}^{m} \log_2 \left[\det \left(\mathbf{I}_{N_r} + \frac{SNR}{N_t} \frac{\mathbf{H}_i \mathbf{H}_i^{\dagger}}{N_{F_i}^2} \right) \right] \qquad (9)$$

where m was the total number of sub-carriers. Since the channel was characterized over a broad frequency band, the capacity of

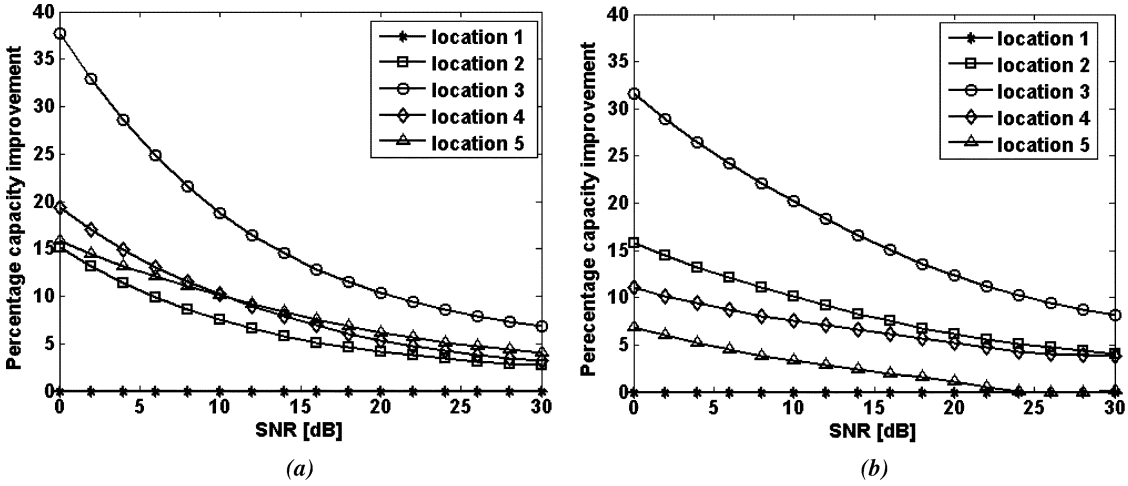

Fig. 17. Percentage capacity improvement versus SNR for 5 different receiver locations in indoor environment for a narrow-band channel at 2.48 GHz: (a) results from measurements, (b) results from simulations.

the wideband channel was defined as an average of the capacities over all the m sub-carriers of the MIMO-OFDM link [37] and the optimal solution for the reconfigurable antenna was the one which guaranteed the highest average capacity.

In Fig. 16 the percentage improvement in channel capacity, achieved with the novel reconfigurable antenna array with respect to a system where a fixed "short" configuration was used for every antenna array element at both transmitter and receiver, was plotted versus different SNR values for all 5 receiver locations. At each location the capacity improvement was defined as the difference in capacity between the best configuration between the sixteen possible configurations (i.e. reconfiguring both transmit and receive arrays) of the reconfigurable antenna system and a 2×2 MIMO system with fixed, "short" configuration antennas. In order to define a "relative" improvement, the channel capacity improvement was normalized for each location with respect to the capacity measured with the "short" configuration antennas. Fig. 16 shows that the reconfigurable antenna solution increased MIMO link capacity with respect to a conventional, fixed antenna system. Only for receiver position 1 there was no improvement since, in that location, the best configuration of the reconfigurable antenna corresponded to the reference "short" configuration. On average, the novel antenna solution achieved a 10% improvement in capacity (with a peak of 28%) for a SNR of 10 dB and 8% (with a peak of 16%) for a SNR of 20 dB with respect to a system with a fixed antenna configuration. Fig. 16 also shows how the improvement in capacity achieved with this novel antenna solution varied with receiver location and so with the particular multipath environment, as previously verified with simulations in Sections IV and V.

A narrowband analysis of the channel, like the MIMO clustered channel model analysis (Section IV), could be performed by considering the channel on each OFDM sub-carrier to be an independent narrowband channel realization. This technique allows for a total of 260 narrowband channel realizations (5 locations times 52 sub-carriers for each location). For this narrowband analysis, results were shown in terms of the capacity CDF. In Fig. 13(b) it was shown how the results from measurements were comparable to the results obtained from the simulation [see Fig. 13(a)] confirming the improvement that the reconfigurable MIMO antenna solution achieved in terms of capacity.

In Fig. 17 is then shown the percentage improvement in capacity achievable with the reconfigurable antenna in a narrowband channel for an indoor environment. The percentage improvement is defined in the same way as in Fig. 16, but it is calculated for a single subcarrier centered at 2.48 GHz. In Fig. 17 the percentage improvement obtained through measurements for the five different locations of the receiver [see Fig. 17(a)] is compared with the one achieved through ray-tracing simulations conducted using FASANT, as in Section V, for the same five locations and for the same frequency of 2.48 GHz [Fig. 17(b)]. The results show a substantial agreement between the measured and the simulated results, confirming therefore the benefit of using the proposed reconfigurable antenna in indoor environments.

VII. Conclusion

A MIMO system using a reconfigurable antenna was introduced and analyzed in terms of capacity. The variation in the antenna geometry and in the mutual coupling effect between the radiating elements was exploited in order to generate different radiation patterns. This pattern diversity was then exploited on a channel by channel basis to identify the antenna configuration which provided the greatest level of channel capacity.

The benefits deriving from using a reconfigurable MIMO antenna system was first motivated through a spatial correlation coefficient analysis in a clustered MIMO channel model. Through this analysis we demonstrated the advantage of switching between different antenna configurations based on the spatial characteristics of the MIMO channel.

Channel capacity was simulated using computational electromagnetics in an outdoor environment and was also computed taking indoor field measurements with a 2×2 MIMO system. Results have shown how the reconfigurable antenna solution described in this paper could provide an average improvement in capacity, for a SNR of 10 dB and 20 dB, of 10% and 8% respectively in a 2×2 MIMO link with respect to a system which did not have this reconfiguration property.

The reconfigurable antenna for MIMO systems is an attractive solution for handheld devices (where space is an important constraint) to maintain good communication link capacity. The proposed antenna is an initial demonstration of reconfigurable MIMO system with only two switches per antenna array element. Future research in this field can then be envisioned in: i) developing novel antenna solutions with higher level of reconfigurability to achieve higher capacity improvement; ii) studying techniques for integrating a switch configuration selection process into practical MIMO-aware ad hoc network nodes; and iii) determining the interval of time over which a switch configuration is optimal before a new configuration needs to be selected.

ACKNOWLEDGMENT

National Instruments has provided equipment donations supporting this work. The authors would like to thank R. Spring, L. Chao, and A. S. Khemka for their helpful comments and suggestions concerning this work.

REFERENCES

[1] G. J. Foschini and M. J. Gans, "On limits of wireless communications in a fading environment when using multiple antennas," *Wireless Personal Commun.*, vol. 6, no. 3, pp. 311–335, 1998.

[2] A. F. Molisch, M. Steinbauer, M. Toeltsch, E. Bonek, and R. S. Thoma, "Capacity of MIMO systems based on measured wireless channels," *IEEE J. Sel. Areas Commun.*, vol. 20, no. 3, pp. 561–569, 2002.

[3] V. Tarokh, N. Seshadri, and A. R. Calderbank, "Space-time codes for high data rate wireless communication: Performance criterion and code construction," *IEEE Trans. Inf. Theory*, vol. 44, no. 2, pp. 744–765, 1998.

[4] T. Svantesson, "An antenna solution for MIMO channels: The multimode antenna," in *Conf. Record of the Asilomar Conf. on Signals, Systems and Computers*, 2000, vol. 2, pp. 1617–1621.

[5] C. B. Dietrich, Jr., K. Dietze, J. R. Nealy, and W. L. Stutzman, "Spatial, polarization, and pattern diversity for wireless handheld terminals," *IEEE Trans. Antennas Propag.*, vol. 49, no. 9, pp. 1271–1281, 2001.

[6] J. P. Kermoal, L. Schumacher, P. E. Mogensen, and K. I. Pedersen, "Experimental investigation of correlation properties of MIMO radio channels for indoor picocell scenarios," in *Proc. IEEE Vehicular Technology Conf.*, 2000, vol. 1, no. 52D, pp. 14–21.

[7] T. Svantesson and A. Ranheim, "Mutual coupling effects on the capacity of multielement antenna systems," in *Proc. IEEE Int. Conf. on Acoustics, Speech and Signal Processing ICASSP*, 2001, vol. 4, pp. 2485–2488.

[8] A. Forenza and R. W. Heath, Jr., "Benefit of pattern diversity via two-element array of circular patch antennas in indoor clustered MIMO channels," *IEEE Trans. Commun.*, vol. 54, no. 5, pp. 943–954, 2006.

[9] W. H. Weedon, W. J. Payne, and G. M. Rebeiz, "MEMS-switched reconfigurable antennas," in *IEEE Antennas and Propagation Society, AP-S Int. Symp. Digest*, 2001, vol. 3, pp. 654–657.

[10] G. H. Huff, J. Feng, S. Zhang, and J. T. Bernhard, "A novel radiation pattern and frequency reconfigurable single turn square spiral microstrip antenna," *IEEE Microw. Wireless Compon. Lett.*, vol. 13, no. 2, pp. 57–59, 2003.

[11] B. A. Cetiner, H. Jafarkhani, J. Y. Qian, H. J. Yoo, A. Grau, and F. De Flaviis, "Multifunctional reconfigurable MEMS integrated antennas for adaptive MIMO systems," *IEEE Commun. Mag.*, vol. 42, no. 12, pp. 62–70, 2004.

[12] B. A. Cetiner, J. Y. Qian, G. P. Li, and F. De Flaviis, "A reconfigurable spiral antenna for adaptive MIMO systems," *Eurasip J. Wireless Commun. Networking*, vol. 2005, no. 3, pp. 382–389, 2005.

[13] B. A. Cetiner, E. Akay, E. Sengul, and E. Ayanoglu, "A MIMO system with multifunctional reconfigurable antennas," *IEEE Antennas Wireless Propag. Lett.*, vol. 5, no. 12, pp. 463–466, 2006.

[14] M. Wennstrom and T. Svantesson, "An antenna solution for MIMO channels: The switched parasitic antenna," in *Proc. IEEE Int. Symp. on Personal, Indoor and Mobile Radio Communications, PIMRC*, 2001, vol. 1, pp. 159–163.

[15] V. Erceg *et al.*, TGn Channel Models IEEE 802.11-03/940r4, 2004.

[16] H. Ozcelik, M. Herdin, W. Weichselberger, J. Wallace, and E. Bonek, "Deficiencies of 'Kronecker' MIMO radio channel model," *Electron. Lett.*, vol. 39, no. 16, pp. 1209–1210, 2003.

[17] S. Wyne, A. F. Molisch, P. Almers, G. Eriksson, J. Karedal, and F. Tufvesson, "Statistical evaluation of outdoor-to-indoor office MIMO measurements at 5.2 GHz," in *IEEE Vehicular Technology Conf.*, 2005, vol. 61, no. 1, pp. 146–150.

[18] C. Oestges, E. Ozcelik, and H. Bonek, "On the prectical use of analytical MIMO channel models," in *IEEE Antennas and Propagation Society Int. Symp.*, 2005, vol. 3B, pp. 406–409.

[19] K. R. Dandekar, G. Xu, and H. Ling, "Computational electromagnetic simulation of smart antenna systems in urban microcellular environments," *IEEE Trans. Veh. Technol.*, vol. 52, no. 4, pp. 733–742, 2003.

[20] M. Jankiraman, *Space Time Codes and MIMO Systems*. Boston, MA: Artech House, 2004.

[21] J. P. Kermoal, L. Schumacher, K. I. Pedersen, P. E. Mogensen, and F. Frederiksen, "A stochastic MIMO radio channel model with experimental validation," *IEEE J. Sel. Areas Commun.*, vol. 20, no. 6, pp. 1211–1226, 2002.

[22] D.-S. Shiu, G. J. Foschini, M. J. Gans, and J. M. Kahn, "Fading correlation and its effect on the capacity of multielement antenna systems," *IEEE Trans. Commun.*, vol. 48, no. 3, pp. 502–513, 2000.

[23] A. Forenza, G. Wan, and R. W. Heath, Jr., "Optimization of 2-element arrays of circular patch antennas in spatially correlated MIMO channels," presented at the IEEE Int. Waveform Diversity and Design Conf., Jan. 23–27, 2006.

[24] H. R. Chuang and L. C. Kuo, "3-D FDTD design analysis of a 2.4-GHz polarization-diversity printed dipole antenna with integrated balun and polarization-switching circuit for WLAN and wireless communication applications," *IEEE Trans. Microw. Theory Tech.*, vol. 51, no. 2 I, pp. 374–381, 2003.

[25] C. A. Balanis, *Antenna Theory: Analysis and Design*. New York: Wiley, 1997.

[26] D. B. Davidson, I. P. Theron, U. Jakobus, F. M. Landstorfer, F. J. C. Meyer, J. Mostert, and J. J. van Tonder, "Recent progress on the antenna simulation program FEKO," in *Proc. South African Symp. on Communications and Signal Processing, COMSIG*, 1998, pp. 427–430.

[27] M. L. Morris and M. A. Jensen, "Network model for MIMO systems with coupled antennas and noisy amplifiers," *IEEE Trans. Antennas Propag.*, vol. 53, no. 1, pt. II, pp. 545–552, 2005.

[28] R. G. Vaughan and J. B. Andersen, "Antenna diversity in mobile communications," *IEEE Trans. Veh. Technol.*, vol. T-36, no. 4, pp. 149–172, 1987.

[29] M. A. Jensen and Y. Rahmat-Samii, "Performance analysis of antennas for hand-held transceivers using FDTD," *IEEE Trans. Antennas Propag.*, vol. 42, no. 8, pp. 1106–1112, 1994.

[30] P. Soma, D. S. Baum, V. Erceg, R. Krishnamoorthy, and A. J. Paulraj, "Analysis and modeling of multiple-input multiple-output (MIMO) radio channel based on outdoor measurements conducted at 2.5 GHz for fixed BWA applications," in *Proc. IEEE Int. Conf. on Communications*, 2002, vol. 1, pp. 272–276.

[31] L. M. Correia, *Wireless Flexible Personalized Communications*. New York: Wiley, 2001.

[32] H. Shin and J. H. Lee, "Capacity of multiple-antenna fading channels: Spatial fading correlation, double scattering, and keyhole," *IEEE Trans. Inf. Theory*, vol. 49, no. 10, pp. 2636–2647, 2003.

[33] M. F. Catedra, J. Perez, A. Gonzalez, O. Gutierrez, and F. Saez de Adana, "Fast computer tool for the analysis of propagation in urban cells," in *Proc. Annual Wireless Communications Conf.*, 1997, pp. 240–245.

[34] J. Perez, J. Ibanez, L. Vielva, and I. Santamaria, "Capacity estimation of polarization-diversity MIMO systems in urban microcellular environments," in *IEEE Int. Symp. on Personal, Indoor and Mobile Radio Communications, PIMRC*, 2004, vol. 4, pp. 2730–2734.

[35] M. A. Jensen and J. W. Wallace, "A review of antennas and propagation for MIMO wireless communications," *IEEE Trans. Antennas Propag.*, vol. 52, no. 11, pp. 2810–2824, 2004.

[36] J. W. Wallace, M. A. Jensen, A. L. Swindlehurst, and B. D. Jeffs, "Experimental characterization of the MIMO wireless channel: Data acquisition and analysis," *IEEE Trans. Wireless Commun.*, vol. 2, no. 2, pp. 335–343, 2003.

[37] H. Bolcskei, D. Gesbert, and A. J. Paulraj, "On the capacity of OFDM-based spatial multiplexing systems," *IEEE Trans. Commun.*, vol. 50, no. 2, pp. 225–234, 2002.

Daniele Piazza (S'03) received the B.S. and Laurea (with high honors) degrees in telecommunication engineering from the Politecnico di Milano, Italy, in 2003 and 2006, respectively, and the M.S. degree in electrical and computer engineering from Drexel University, Philadelphia, PA, in 2006, where he is currently working toward the Ph.D. degree.

While working toward the M.S. degree at Drexel University, he conducted research focused on reconfigurable antennas for MIMO communications and is currently developing reconfigurable antenna systems for adaptive MIMO communications. He is also working as a researcher at Politecnico di Milano in the field of radio frequency identification (RFId). His research interests concentrate mainly on reconfigurable antennas, smart antenna arrays, MIMO communications and RFId systems.

Nicholas J. Kirsch (S'00) received the B.S. degree in electrical engineering from the University of Wisconsin-Madison, in 2003 and the M.S. degree in telecommunications engineering from Drexel University, Philadelphia, PA, in 2006, where he is currently working toward the Ph.D. degree.

From 2001 to 2002, he worked at W. L. Gore & Associates on fiber optic link modules and long-wavelength lasers. His research interests include MIMO communication systems, ad hoc networking, adaptive radio systems, and reconfigurable antennas.

Antonio Forenza (S'04–M'06) received the M.S. degree in telecommunications engineering from the Politecnico di Torino, Italy, and the Eurecom Institute, Sophia Antipolis, France, in 2001, and the Ph.D. degree in electrical and computer engineering from the University of Texas at Austin, in 2006.

In 2001, he interned as a Systems Engineer at Iospan Wireless, Inc., San Jose, CA, a startup company that developed the first commercial MIMO-OFDM communication system. His main research focus was on link-adaptation and physical layer algorithm design. In fall 2001, he joined ArrayComm, Inc., San Jose, CA, as a Systems Engineer. In ArrayComm, he was actively involved in the design and implementation of smart antenna systems for the 3G WCDMA wireless platform. During summers 2004 and 2005, he interned as a Research Engineer at Samsung Advanced Institute of Technology (SAIT), Suwon, Korea, and Freescale Semiconductor, Inc., Austin, TX, respectively, developing adaptive MIMO transmission and MU-MIMO precoding techniques for 3GPP, IEEE 802.11n and IEEE 802.16e standards systems. Since June 2006, he has been working for Rearden, LLC, San Francisco, CA, as a Senior Systems Engineer. His research interests include MIMO antenna design, adaptive MIMO transmission techniques, precoding methods for MU-MIMO, smart antenna signal processing.

Robert W. Heath, Jr. (S'96–M'01–SM'06) received the B.S. and M.S. degrees from the University of Virginia, Charlottesville, in 1996 and 1997, respectively, and the Ph.D. from Stanford University, Stanford, CA, in 2002, all in electrical engineering.

From 1998 to 2001, he was a Senior Member of the Technical Staff then a Senior Consultant at Iospan Wireless Inc, San Jose, CA, where he worked on the design and implementation of the physical and link layers of the first commercial MIMO-OFDM communication system. In 2003, he founded MIMO Wireless Inc., a consulting company dedicated to the advancement of MIMO technology. Since January 2002, he has been with the Department of Electrical and Computer Engineering, the University of Texas at Austin, where he is currently an Associate Professor and member of the Wireless Networking and Communications Group. His research interests cover a broad range of MIMO communication including limited feedback techniques, multihop networking, multiuser MIMO, antenna design, and scheduling algorithms as well as 60 GHz communication techniques.

Dr. Heath is the recipient of the David and Doris Lybarger Endowed Faculty Fellowship in Engineering. He was an Editor for the IEEE TRANSACTIONS ON COMMUNICATION and an Associate Editor for the IEEE TRANSACTIONS ON VEHICULAR TECHNOLOGY. He is a member of the Signal Processing for Communications Technical Committee in the IEEE Signal Processing Society. He was a technical Co-Chair for the 2007 Fall Vehicular Technology Conference, and is the organizer of the 2008 Communication Theory Workshop, and a Co-Organizer of the 2009 Signal Processing for Wireless Communications Workshop.

Kapil R. Dandekar (S'95–M'01–SM'07) received the B.S. degree in electrical engineering from the University of Virginia, Charlottesville, in 1997 and the M.S. and Ph.D. degrees in electrical and computer engineering from the University of Texas at Austin, in 1998 and 2001, respectively.

In 1992, he worked at the U.S. Naval Observatory and from 1993 to 1997, he worked at the U.S. Naval Research Laboratory. In 2001, he joined the Electrical and Computer Engineering Department, Drexel University, Philadelphia, PA, as an Assistant Professor. He is currently the Director of the Drexel Wireless Systems Laboratory (DWSL), which has been supported by the U.S. National Science Foundation, Army CERDEC, National Security Agency, Office of Naval Research, and private industry. His current research interests involve MIMO ad hoc networks, reconfigurable antennas, free space optical communications, ultrasonic communications, and sensor networks. He has published articles in several journals including the IEEE TRANSACTIONS ON ANTENNAS AND PROPAGATION, IEEE TRANSACTIONS ON WIRELESS COMMUNICATIONS, IEEE TRANSACTIONS ON COMMUNICATIONS, IEEE TRANSACTIONS ON VEHICULAR TECHNOLOGY, and *IEE Electronics Letters*.

Dr. Dandekar currently serves on the editorial board of IEEE Expert Now and serves on the Pre-University Education Committee of the IEEE Educational Activities Board. He is a continuing active member of the Technical Program Committee for the IEEE Radio and Wireless Symposium. He served as an Associate Editor for the IEEE TRANSACTIONS ON VEHICULAR TECHNOLOGY and is currently the Chairman of the Philadelphia chapter of the IEEE Vehicular Technology Society.